

ACCEPTED MANUSCRIPT • OPEN ACCESS

Bend monitoring and refractive index sensing using flat fibre and multicore Bragg gratings

To cite this article before publication: Christopher Holmes *et al* 2020 *Meas. Sci. Technol.* in press <https://doi.org/10.1088/1361-6501/ab8710>

Manuscript version: Accepted Manuscript

Accepted Manuscript is “the version of the article accepted for publication including all changes made as a result of the peer review process, and which may also include the addition to the article by IOP Publishing of a header, an article ID, a cover sheet and/or an ‘Accepted Manuscript’ watermark, but excluding any other editing, typesetting or other changes made by IOP Publishing and/or its licensors”

This Accepted Manuscript is © 2020 The Author(s). Published by IOP Publishing Ltd..

As the Version of Record of this article is going to be / has been published on a gold open access basis under a CC BY 3.0 licence, this Accepted Manuscript is available for reuse under a CC BY 3.0 licence immediately.

Everyone is permitted to use all or part of the original content in this article, provided that they adhere to all the terms of the licence <https://creativecommons.org/licenses/by/3.0>

Although reasonable endeavours have been taken to obtain all necessary permissions from third parties to include their copyrighted content within this article, their full citation and copyright line may not be present in this Accepted Manuscript version. Before using any content from this article, please refer to the Version of Record on IOPscience once published for full citation and copyright details, as permissions may be required. All third party content is fully copyright protected and is not published on a gold open access basis under a CC BY licence, unless that is specifically stated in the figure caption in the Version of Record.

View the [article online](#) for updates and enhancements.

Bend Monitoring and Refractive Index Sensing using Flat Fibre and Multicore Bragg gratings

Christopher Holmes¹, Sumiaty Ambran² Peter A Cooper¹, Andrew S Webb¹, James C Gates¹, Corin BE Gawith¹, Jayanta K Sahu¹ and Peter GR Smith¹

¹ Optoelectronics Research Centre, University of Southampton, Southampton, SO17 1BJ
² Malaysia-Japan International Institute of Technology, Universiti Teknologi Malaysia, Kuala Lumpur

E-mail: christopher.holmes@soton.ac.uk

Received xxxxxx
Accepted for publication xxxxxx
Published xxxxxx

Abstract

A planarized optical fibre designed for 2-dimensional bend monitoring and external refractive index sensing is presented. The approach uses two singlemode waveguides each containing a set of spectrally multiplexed Bragg gratings. To achieve sensitivity to bending and external refractive index the cladding material of the fibre is partially removed through physical machining. This acts to offset the neutral axis, increasing bend sensitivity and exposes the evanescent field of the guided mode permitting external refractive index monitoring. Through collective monitoring of the Bragg grating array real time, multiparameter sensing is attainable allowing new capability for intelligent monitoring.

Keywords: optical fibre, Bragg gratings, multicore fibre, planar optics, bend sensing

1. Introduction

Intelligent monitoring of engineered structures and materials is enabled by increasing both the number of sensor elements and the capability of the sensor technology [1]. Optical fibre sensors have specific advantages when applied to intelligent monitoring as they have: immunity to electromagnetic interference; are lightweight; have a small cross-sectional footprint; broad spectral bandwidth; remote and secure connectivity and use materials that are typically chemically inert and non-conductive. Multiparameter optical fibre sensors are an enabler for intelligent monitoring, as they provide an increased sensor capability. They have been the subject of considerable research in recent years [2] as they can additionally improve the accuracy and precision of multi-variant system measurements. For example, through simultaneous temperature monitoring, refractive index sensing can be thermally compensated improving accuracy and precision. Previous work on multiparameter optical fibre bend monitoring has included multicore fibre [3], [4] and

regular fibre adhered to larger cantilevered structures. In both instances the neutral axis is offset from a waveguide core to make it optically responsive to bending. Multiparameter bend monitoring has also been demonstrated in flexible planar optical platforms, notably silica [5], [6], polymer [7], chalcogenide [8]–[10] and silicon [11]. In these configurations strain is mapped for a 2-dimensional plane.

The work reported here uniquely considers a flexible planar optical fibre platform, termed flat fibre [12], illustrated in Figure 1. Flat fibre provides both long flexible lengths associated with optical fibre and the functionality of planar optics. Recent applications for flat fibre have included refractometry and dosimetry. Refractometry has included guided mode [13], leaky mode [14] and plasmon coupling [15], [16] techniques. Dosimetry has included in-vivo applications, through use of thermoluminescence [17], [18]. None of this work has yet considered bend monitoring or utilisation of multiparameter sensing.

Flat fibre is an inherent slab waveguide, laterally multimode and vertically single mode [12]. Through use of

physical micromachining [19], Direct UV writing (DUW) [13] or Femtosecond laser writing [20], [21] these multimode characteristics can be manipulated. Through direct laser writing (either DUW or Femtosecond writing) multiple single mode waveguides can be arbitrarily positioned into the core layer of flat fibre. In this instance flat fibre shares similarity to solid multicore fibre [22], with the distinguishing advantage of integrated circuitry [23].

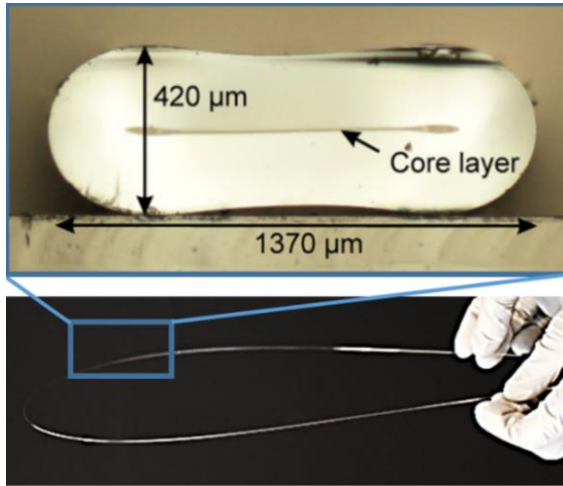


Figure 1. Flexible flat optical fibre, illustrating the planar cross-section (top) and inherent flexibility (bottom).

This report describes the design, fabrication and response of a flat fibre capable of multiparameter sensing, namely monitoring two-dimensional bending, external refractive index and temperature. Bend sensitivity of flat fibre is directly compared to multicore cylindrical fibre through replicating dual-axis bending described by Flockhart *et al* [24].

2. Design Concept and Fabrication

Flat fiber is fabricated using modified chemical vapour deposition (MCVD) and fiber drawing. The process differs from standard optical fibre fabrication only at the drawing stage, where a vacuum is applied to the preform in order to preferentially collapse it into a planar geometry. A cross-section of the resulting fibre is shown in Figure 1.

The strain observed in the core layer of flat fibre is dependent upon the bending moments applied and relative position from the neutral axis. For bending moments about the y-axis, M_y , the neutral axis is located upon the plane of symmetry, as shown in Figure 2 (a). For bending moments about the x-axis, M_x , the neutral axis overlaps with the core layer, illustrated in Figure 2 (b). This means that for bending in the x-axis there is minimal strain observed in the core. The partial removal of cladding material on one side of the flat fibre acts to offset the neutral axis, as shown in Figure 2 (c), meaning strain induced bending for the M_x can be observed. Further to this, complete removal of clad material will permit

evanescent field exposure of the guided modes, which can be leveraged to probe external refractive index.

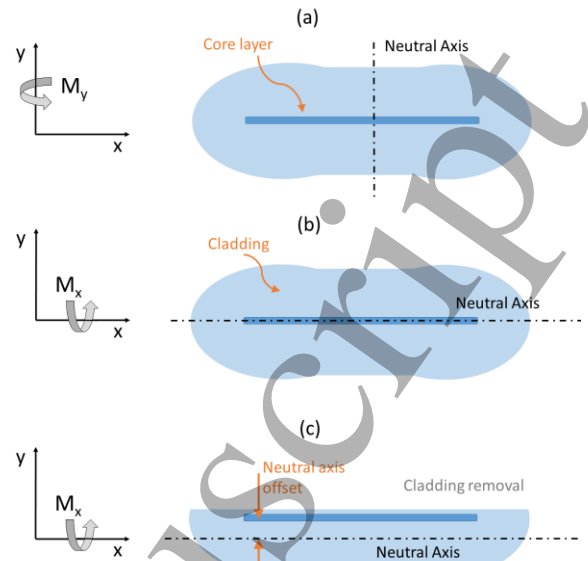


Figure 2. Neutral axis locations in flat fibre (cross section) for (a) bending moments about the y-axis (b) bending moments about the x-axis (c) bending moments about the x-axis, with partial removal of clad material removed.

To offset the neutral axis cladding material was removed through physical machining, achieved through post process lapping and polishing (using a Logitech LP50). The physical machining process allowed a small wedge angle of 0.27° between the top and bottom of the fibre, shown in Figure 3 (a). This meant that the overlaid thickness varied from $105\mu\text{m}$ at the thickest end to complete removal of the core layer at the opposite end. It also meant that part of the flat fibre was evanescently exposed to its external environment.

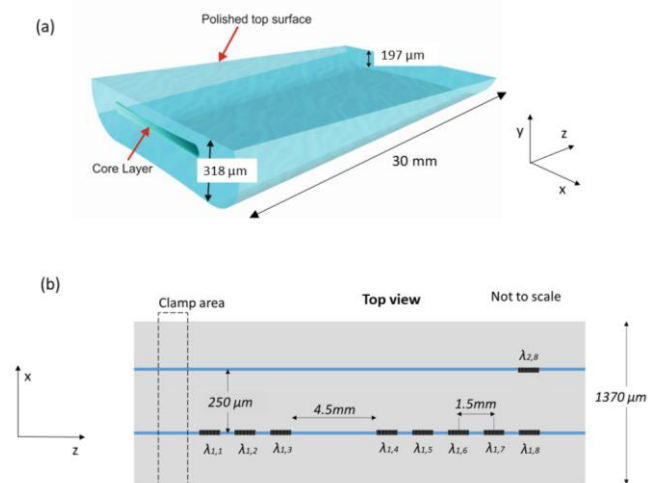


Figure 3. Configuration of physically machined flat fibre showing (a) the location of direct UV written waveguides and Bragg gratings and (b) the machined wedge used to shift the neutral axis.

To allow fibre bending, refractive index and temperature measurements two waveguides containing an array of spectrally multiplexed Bragg gratings were defined, as outlined in Figure 3(b). The waveguides and Bragg gratings were written into the photosensitive Germanium doped core layer of the flat fibre, through use of small spot direct UV writing [25]. Here, a 244-nm frequency doubled argon-ion laser is used to increase the local refractive index in the core layer. A $6\mu\text{m}$ spot consisting of two coherent beams focused and overlapping are translated through the fibre. The dual beams create an inherent interference pattern, which was amplitude modulated during translation in order to define the outlined array of multiplexed Bragg gratings and waveguides. Through use of a commercial optical backscatter reflectometer (Luna, OBR 4400 series) waveguide propagation loss was measured to be 0.09 ± 0.01 dB/cm.

Direct UV writing of the waveguides and gratings were made prior to the physical machining of the fibre. The two straight waveguides defined were offset by $125\mu\text{m}$ and centred about the vertical neutral axis (i.e. $250\mu\text{m}$ from each other), shown in Figure 3(b).

3. Bend sensitivity of flat fibre

Bending of the flat fibre was induced through leveraging it as a cantilever. The arrangement clamped the thickest end of fibre, with packed borosilicate slides and epoxy, as illustrated in Figure 4. Light was coupled into the two flat fibre waveguides using two single mode fibres (SMF). The arrangement used a two-port SMF pigtail, consisting of two silicon v-grooves of pitch $250\mu\text{m}$ (OzOptics).

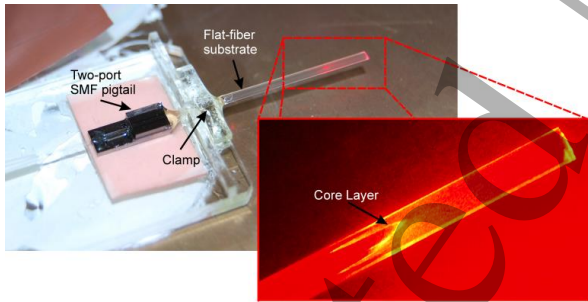


Figure 4. Flat fibre cantilevered section, showing optical coupling of 633nm laser light.

The cantilevered arrangement was clamped down and deflected at the end about y-axis and x-axis respectively. This was achieved using a lever and multi-axis micrometre translation stages, as illustrated in Figure 5(a). The Bragg gratings in each waveguide were simultaneously addressed using two Optical Spectrum Analysers, OSAs (ANDO AQ6317B) and a 5 element superluminescent LED broadband source (Amonics ASLD-CWDM-5-B-FA), using the configuration shown in Figure 5(b). Back reflected spectral signatures are presented in Figure 6.

To theoretically corroborate the optical response, the strain induced in flat fibre was modelled through finite element analysis (FEA) (Comsol Multiphysics, Solid Mechanics). This considered all three orthogonal linear strain components [5].

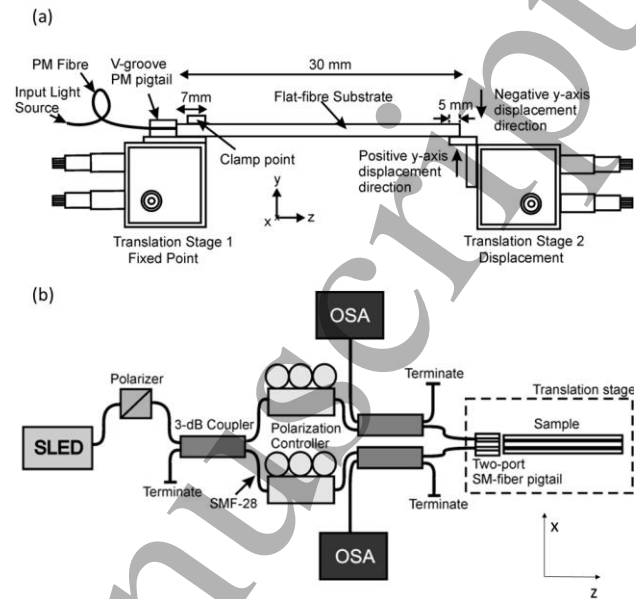


Figure 5. Bend test set-up, showing (a) translation stage arrangement and (b) optical characterisation set-up.

Figure 6 depicts the measured spectral response for the Bragg grating array, subjected to a -1 mm y-axis deflection. Here, grating position is referenced with respect to the cantilever's root. Unlike a cantilever of uniform cross section where maximum strain would occur at the root, this cantilever has variable cross-section thus a varying neutral axis and stiffness along the length. This means that the maximum spectral shift occurs at the distal end of the cantilever, observed both experimentally and with FEA simulations.

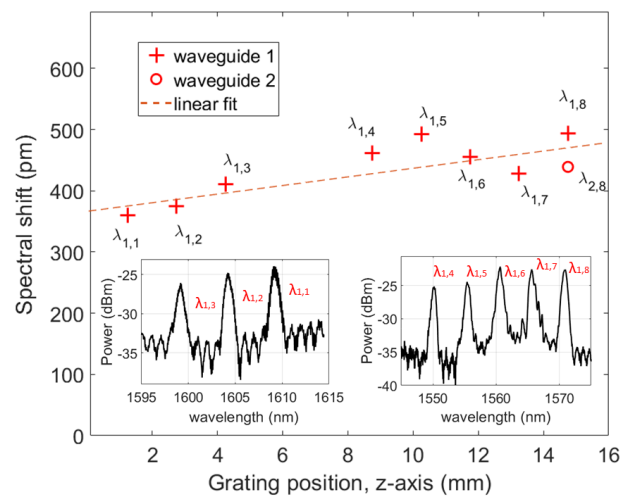


Figure 6. Spectral response for Bragg gratings along the length of flat optical fibre, upon a distal end deflection of 1 mm in the y-axis, (inserts) corresponding reflection spectra from gratings.

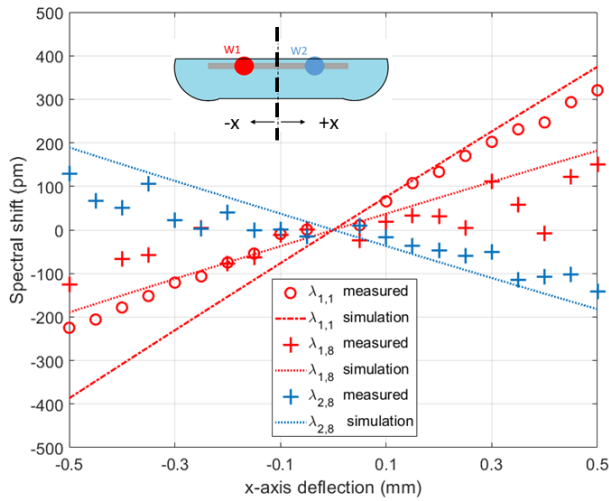


Figure 7. Spectral response of Bragg gratings at the root and distal end of flat fibre subjected to calibrated deflections in the x-axis.

Figures 7 and 8 show the Bragg responses for gratings at the distal end and root of the cantilever, subjected to x-axis and y-axis displacements. Experimental observations are in good agreement with theoretical simulation. However, response asymmetries about zero-deflection exist. This is believed to result from a small variation of thickness along the x-axis. It should be noted that this would be most notable for x-axis deflection due to a neutral axis offset, as indeed observed. Bend sensitivity for the Bragg gratings are summarised in Table 1. A maximum of 641 ± 5 pm/mm occurs for positive deflections about the x-axis, inferred from 10 data points. This is approximately an order of magnitude larger in spectral shift when compared to similar work on multicore optical fibre [24]. It is noted that the neutral axis offset is approximately 6 times larger in this work and therefore a larger spectral response is indeed expected.

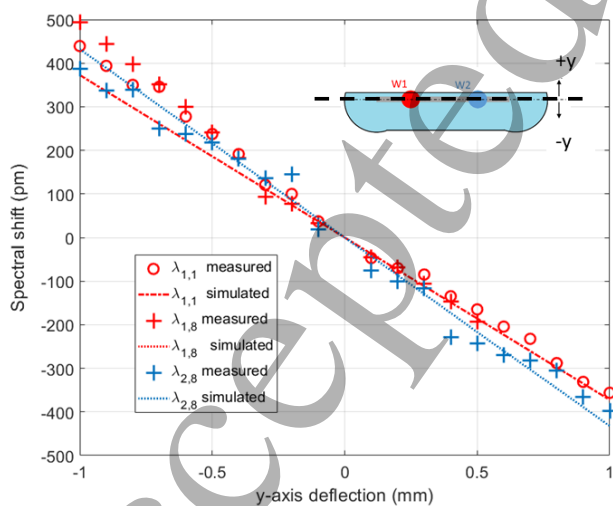


Figure 8. Spectral response of Bragg gratings at the root and distal end of flat fibre subjected to calibrated deflections in the y-axis.

Bragg grating	x-axis deflection (pm/mm)	y-axis deflection (pm/mm)
$\lambda_{1,1}$	280 ± 50	-400 ± 40
$\lambda_{1,8}$	641 ± 5	-490 ± 50
$\lambda_{2,8}$	-240 ± 10	-387 ± 3

Table 1. Summarised bend sensitivity

The thermo-optic response for the Bragg gratings was calibrated from 22°C to 58°C, using a hotplate (Fisher Scientific, Isotemp) and K-type thermocouple. Thermal sensitivity was measured to be 8.5 ± 0.6 pm/K for the evanescent exposed ($\lambda_{2,8}$) Bragg grating, and 11.6 ± 0.7 pm/K for the none exposed gratings. It is noted that upon the calibration of thermal and bending response of three gratings, temperature can be practically deduced through use of linear simultaneous equations.

3. Refractive index sensitivity of flat fibre

One of the Bragg gratings in the array, $\lambda_{2,8}$, was evanescently exposed and responded to changes in external refractive index. It is noted that due to the secondary wedge along the x-axis only this grating displayed such sensitivity. To calibrate the response, the fibre was tested with calibrated refractive index oils (Cargille Series AAA and Series AA). Figure 9 shows the spectral sensitivity of this grating to the fluids.

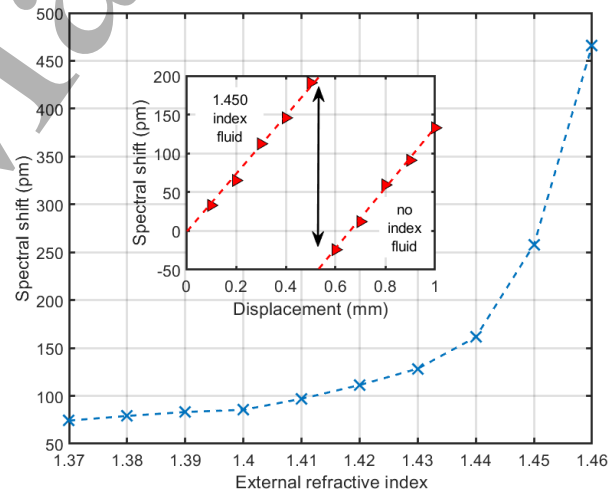


Figure 9. Response of an evanescent field exposed flat optical fibre Bragg grating to Cargille refractive index fluids that are calibrated at 633 nm (insert) vertical bending response of the grating with and without index oil.

The Bragg wavelength changes are larger for external refractive indices approaching that of the core layer, a trend understood from solutions to Helmholtz equations [26]. The maximum sensitivity to external refractive index is 20 nm/riu. It is further observed that in the presence of an external refractive index fluid there is negligible influence on the bend sensitivity, as seen in Figure 9 insert. This shows a unique

capability of flat fibre to simultaneously monitor strain and external refractive index, distinguishable through differential spectral measurements.

4. Discussion

This work is the first demonstration of combined bend and external refractive index monitoring, using flat fibre. The solution reported uses physical machining in the form of lapping and polishing to both shift the neutral axis and gain partial evanescent field exposure. It is noted that other techniques including laser ablation, wet etching, dry etching, ultrasonic milling either post or prior to fibre drawing could also be used to achieve a similar geometric configuration. These would be a direction for further development and may offer greater scalability.

Monitoring external refractive index in addition to strain components would provide a unique capability for intelligent monitoring. For example, it could be practically used for monitoring degradation of epoxy resin [27], [28] such as that found within advanced composites (e.g. carbon fibre reinforced polymer). This capability could be set alongside traditional Bragg grating strain monitoring capability achieved through embedding optical flat fibre. Applications could also include physical and refractive index monitoring of fluids, which could be used to infer directional fluid flow (through cantilever deflection) and density (through external refractive index).

Flat fibre has an asymmetric stiffness inherent to its geometry. This limits complex 3-dimensional shape sensing, as demonstrated in multicore optical fibre [3], [29]. However, the platform could be embedded within advanced composites or upon a planar surface. Investigation into long-term performance and durability under suitable strain transfer [30] would be required and the subject of future investigation.

5. Conclusion

This is the first report of multi-parameter sensing within flat fibre. The platform demonstrates two-dimensional bend sensitivity and combined external refractive index monitoring and temperature sensing.

The measured bend sensitivity concurs with theoretical models and is enabled through physical machining of the fibre. A maximum bend sensitivity of 641 ± 5 pm/mm was measured and external refractive index sensitivity of 20 nm/riu.

Flat fibre enables multiparameter sensing capability, through which data-rich information can be generated with potential application for future intelligent monitoring applications.

References

- [1] M. A. McEvoy and N. Correll, "Materials that couple sensing, actuation, computation, and communication," *Science* (80-.), vol. 347, no. 6228, pp. 1328–1337, 2015.
- [2] S. Pevec and D. Donlagić, "Multiparameter fiber-optic sensors: a review," *Opt. Eng.*, vol. 58, no. 07, p. 1, 2019.
- [3] J. P. Moore and M. D. Rogge, "Shape sensing using multi-core fiber optic cable and parametric curve solutions," *Opt. Express*, vol. 20, no. 3, p. 2967, 2012.
- [4] G. A. Cranch, G. M. H. Flockhart, W. N. MacPherson, J. S. Barton, and C. K. Kirkendall, "Ultra-high-sensitivity two-dimensional bend sensor," *Electron. Lett.*, vol. 42, no. 9, 2006.
- [5] C. Holmes, L. G. Carpenter, H. L. Rogers, J. C. Gates, and P. G. R. Smith, "Quantifying the optical sensitivity of planar Bragg gratings in glass micro-cantilevers to physical deflection," *J. Micromechanics Microengineering*, vol. 21, no. 3, p. 035014, 2011.
- [6] C. Holmes, L. G. Carpenter, J. C. Gates, and P. G. R. Smith, "Miniaturization of Bragg-multiplexed membrane transducers," *J. Micromechanics Microengineering*, vol. 22, no. 2, p. 025017, Feb. 2012.
- [7] J. Missinne *et al.*, "Bragg-grating-based photonic strain and temperature sensor foils realized using imprinting and operating at very near infrared wavelengths," *Sensors (Switzerland)*, vol. 18, no. 8, pp. 1–14, 2018.
- [8] J. Hu, L. Li, H. Lin, P. Zhang, W. Zhou, and Z. Ma, "Flexible integrated photonics: where materials, mechanics and optics meet [Invited]," *Opt. Mater. Express*, vol. 3, no. 9, p. 1313, Aug. 2013.
- [9] L. Li *et al.*, "Monolithically integrated stretchable photonics," *Light Sci. Appl.*, vol. 7, no. 2, p. 17138, 2018.
- [10] L. Li *et al.*, "A new twist on glass: A brittle material enabling flexible integrated photonics," *Int. J. Appl. Glas. Sci.*, vol. 8, no. 1, pp. 61–68, 2017.
- [11] L. Fan, L. T. Varghese, Y. Xuan, J. Wang, B. Niu, and M. Qi, "Direct fabrication of silicon photonic devices on a flexible platform and its application for strain sensing," *Opt. Express*, vol. 20, no. 18, p. 20564, 2012.
- [12] K. D. Dambul *et al.*, "Fabrication and characterization of Ge-doped flat fibres," *J. Mod. Opt.*, vol. 66, no. 11, pp. 1219–1225, 2019.
- [13] F. Rafiq *et al.*, "Direct UV Written Optical Waveguides in Flexible Glass Flat Fiber Chips," *IEEE JOURNAL Sel. TOP. QUANTUM ELECTRON.*, vol. 18, no. 5, pp. 1534–1539, 2012.
- [14] P. S. Yong, T. D. Chai, S. Y. Meng, Y. K. Shien, G. A. Mahdiraji, and F. R. M. Adikan, "Numerical Investigation of Single-mode Operation Flat Fiber and Dispersion," *Procedia Eng.*, vol. 140, pp. 95–98, 2016.
- [15] M. De and V. K. Singh, "Analysis of a highly sensitive flat fiber plasmonic refractive index sensor," *Appl. Opt.*, vol. 59, no. 2, p. 380, 2020.
- [16] A. A. Rifat, G. A. Mahdiraji, Y. M. Sua, R. Ahmed, Y. G. Shee, and F. R. M. Adikan, "Highly sensitive multi-core flat fiber surface plasmon resonance refractive index sensor," *Opt. Express*, vol. 24, no. 3, p. 2485, 2016.
- [17] S. E. Lam, D. A. Bradley, R. Mahmud, M. Pawanchek, H. A. Abdul Rashid, and N. Mohd Noor, "Dosimetric characteristics of fabricated Ge-doped silica optical fibre for small-field dosimetry," *Results Phys.*, vol. 12, no. December 2018, pp. 816–826, 2019.
- [18] M. Ghomeishi, G. A. Mahdiraji, F. R. M. Adikan, N. M. Ung, and D. A. Bradley, "Sensitive Fibre-Based Thermoluminescence Detectors for High Resolution In-Vivo Dosimetry," *Sci. Rep.*, vol. 5, pp. 1–10, 2015.
- [19] S. Ambran *et al.*, "Fabrication of a Multimode Interference Device in a Low-Loss Flat-Fiber Platform Using Physical Micromachining Technique," *J. Light. Technol.*, vol. 30,

- no. 17, pp. 2870–2875, 2012.
- [20] K. Kalli *et al.*, “Flat fibre and femtosecond laser technology as a novel photonic integration platform for optofluidic based biosensing devices and lab-on-chip applications: Current results and future perspectives,” *Sensors Actuators, B Chem.*, vol. 209, pp. 1030–1040, 2015.
- [21] S. J. Beecher, R. R. Thomson, G. Brown, A. S. Webb, J. K. Sahu, and A. K. Kar, “Bragg Grating Waveguide Array Ultrafast Laser Inscribed into the Cladding of a Flat Fiber,” *MATEC Web Conf.*, vol. 8, no. April 2016, p. 06001, 2013.
- [22] D. J. Richardson, J. M. Fini, and L. E. Nelson, “Space-division multiplexing in optical fibres,” *Nat. Photonics*, vol. 7, no. 5, pp. 354–362, 2013.
- [23] A. S. Webb *et al.*, “MCVD planar substrates for UV-written waveguide devices,” *Electron. Lett.*, vol. 43, no. 9, pp. 1–2, 2007.
- [24] G. M. H. Flockhart, W. N. MacPherson, J. S. Barton, L. Zhang, I. Bennion, and J. D. C. Jones, “Two-axis bend measurement with Bragg gratings in multicore optical fiber,” *Opt. Lett.*, vol. 28, no. 6, p. 387, 2007.
- [25] C. Holmes *et al.*, “Direct UV-written planar Bragg grating sensors,” *Meas. Sci. Technol.*, vol. 26, no. 11, p. 112001, 2015.
- [26] A. N. Chryssis, S. M. Lee, S. B. Lee, S. S. Saini, and M. Dagenais, “High sensitivity evanescent field fiber Bragg grating sensor,” *IEEE Photonics Technol. Lett.*, vol. 17, no. 6, pp. 1253–1255, 2005.
- [27] C. Marro Bellot, M. Olivero, M. Sangermano, and M. Salvo, “Towards self-diagnosis composites: Detection of moisture diffusion through epoxy by embedded evanescent wave optical fibre sensors,” *Polym. Test.*, vol. 71, no. September, pp. 248–254, 2018.
- [28] T. Kumar, BG., Singh, RP., Nakamura, “Degradation of Carbon Fiber-reinforced,” *J. Compos. Mater.*, vol. 36, no. 24, pp. 2713–2733, 2002.
- [29] K. K. Mandal *et al.*, “Enhancement of accuracy in shape sensing of surgical needles using optical frequency domain reflectometry in optical fibers,” *Biomed. Opt. Express*, vol. 8, no. 4, p. 2210, 2017.
- [30] H. Wang, P. Xiang, and L. Jiang, “Strain transfer theory of industrialized optical fiber-based sensors in civil engineering: A review on measurement accuracy, design and calibration,” *Sensors Actuators, A Phys.*, vol. 285, pp. 414–426, 2019.